Phase transition in the parametric natural visibility graph

A. A. Snarskii[1,2] and I. V. Bezsudnov[3,*]
[1]*National Technical University of Ukraine "Igor Sikorsky Kyiv Polytechnic Institute", Kiev 03056, Ukraine*
[2]*Institute for Information Recording, NAS Ukraine, Kiev 03113, Ukraine*
[3]*JSC Nauka-Service, Moscow 127473, Russia*

(Received 27 June 2016; revised manuscript received 21 September 2016; published 26 October 2016)

We investigate time series by mapping them to the complex networks using a parametric natural visibility graph (PNVG) algorithm that generates graphs depending on arbitrary continuous parameter—the angle of view. We study the behavior of the relative number of clusters in PNVG near the critical value of the angle of view. Artificial and experimental time series of different nature are used for numerical PNVG investigations to find critical exponents above and below the critical point as well as the exponent in the finite size scaling regime. Altogether, they allow us to find the critical exponent of the correlation length for PNVG. The set of calculated critical exponents satisfies the basic Widom relation. The PNVG is found to demonstrate scaling behavior. Our results reveal the similarity between the behavior of the relative number of clusters in PNVG and the order parameter in the second-order phase transitions theory. We show that the PNVG is another example of a system (in addition to magnetic, percolation, superconductivity, etc.) with observed second-order phase transition

DOI: 10.1103/PhysRevE.94.042137

The study of the time series with complex, fractal structure presently attracts constant interest due to the rich potential of engineering applications that cover a wide range of phenomena from human cardiac rhythm variations to earthquakes and turbulent flow [1–19]. The time series are examined by means of different methods: conventional statistic (averages, dispersions, etc.), power spectra calculations (the presence of the $1/f$ noise, etc.), the fractal dimensional and multifractal analysis, the presence of strange attractors, and the like.

The idea to investigate time series by mapping them to the complex networks (graphs) [20–22] is very attractive. Two advanced research areas are combined under this approach: the methods of the nonlinear time series analysis [23–30] and the theory of the complex networks [31–37]. It becomes possible to apply the rich, well-developed methods of the complex networks analysis to the investigation of the time series with a complicated structure, such as the fractal time series.

Currently there are several algorithms to map time series to the complex network. For instance, it was suggested in [20] to build a network using the proximity of coordinates in the Poincare section of the time series. Another type of algorithms introduces the concept of visibility graph [21]. The algorithm to build the natural visibility graph (NVG) was proposed in [21]. Later in [22] a horizontal visibility graph (HVG) algorithm was described.

The NVG and the HVG algorithms allow us to explore the time series of complex structure associated with a variety of phenomena: fluctuations of turbulent flows, stock market indices, human cardiac dynamic, stochastic and chaotic series, and others [13–19].

The generalization of the NVG algorithm was proposed in [38]. The parametric natural visibility graph (PNVG) algorithm assigns to each link of NVG a weight called the angle of view, the PNVG consists of NVG links with the angle of view less than the given angle of view α. Thus, each α generates a new graph. Therefore, the PNVG algorithm allows us to explore graph properties depending on the angle of view α. The ability to change arbitrarily the angle of view α added to the name of the algorithm the word "parametric," we will denote it also as PNVG(α).

In the present work we demonstrate that properties of PNVG(α) behave similarly to the order parameter and the correlation length in the theory of the second-order phase transitions. Furthermore, to be short, we omit the term "similar to" before all the terms using the phase transitions terminology, for example, instead of "the parameter similar to the critical exponent" we write for short "the critical exponent," etc.

The paper is structured as follows. First, the algorithm to construct the PNVG is described, then PNVG(α) is constructed for a set of artificial and experimental time series and the detail investigation of the relative number of clusters in PNVG(α) is given. Finally, discussions and conclusions are presented.

I. PARAMETRIC NATURAL VISIBILITY GRAPH ALGORITHM

The PNVG mapping algorithm was proposed by authors and described in [38]. To construct the PNVG we use the time series $\{t_i,\ i = 1,\ldots,N\}$, which contains events time stamps, for example, RR peak in the ECG, weather station data, etc., then a series of intervals are generated $\{x(t_i) = t_{i+1} - t_i,\ i = 1,\ldots,N-1\}$. According to the procedure, all $x(t_i)$ values are positive.

Initially the time series is mapped to the NVG [21]. The NVG mapping algorithm is presented schematically in Fig. 1. In the time-interval plane $(t,\ x(t))$ the line segments $\{((t_i,0) - (t_i,x(t_i))),\ i = 1,\ldots,N-1\}$ are plotted, points $(t_i,x(t_i))$ will be treated as positions of NVG nodes on that plane. The link between NVG nodes is considered to exist only if the line connecting corresponding nodes do not cross any line segment between them.

This way of graph constructing (see Fig. 1) allows us to assign to every NVG link a natural temporal direction and a weight equal to the angle between link direction and downward direction; we call it the angle of view. The link of NVG belongs

*Corresponding author: biv@akuan.ru

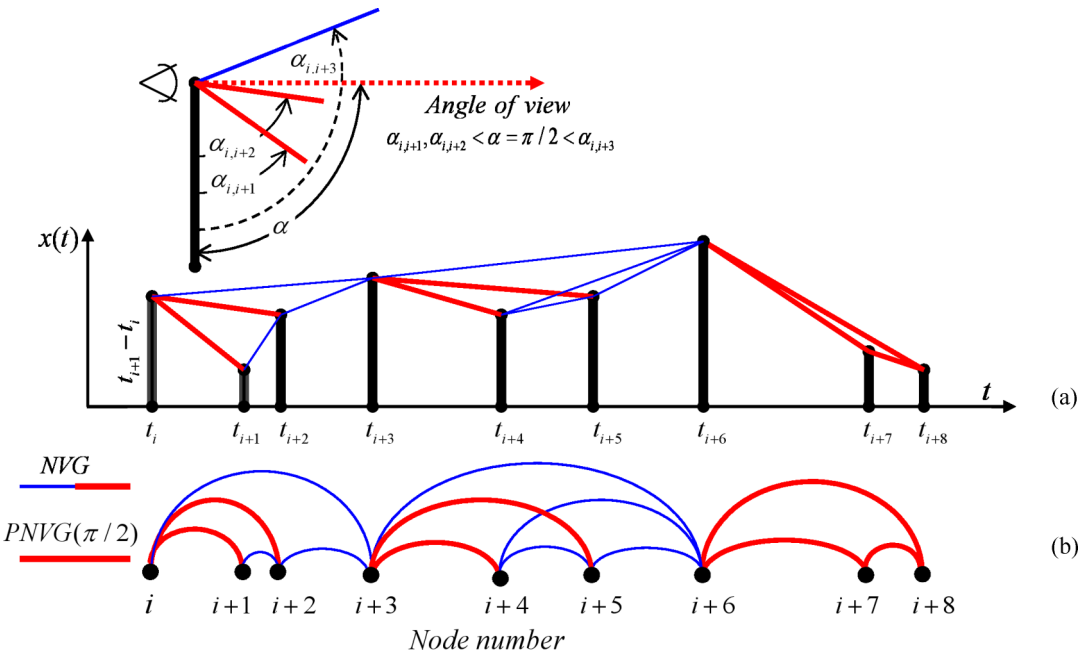

FIG. 1. Parametric natural visibility graph mapping algorithm. (a) PNVG selection criterion demonstration. (b) NVG and PNVG diagram.

to the PNVG if its angle of view is less than the given value of angle of view α.

The PNVG selection criterion for the angle of view $\alpha = \pi/2$ is shown schematically in Fig. 1 top left. NVG links with the angle of view lower than the angle of view $\alpha = \pi/2$ (e.g., $\alpha_{i,i+2}$) are indicated by thick lines, links with angles larger then $\alpha = \pi/2$ (e.g., $\alpha_{i,i+3}$) thin lines. The NVG is composed of both types of links, i.e., thin and thick lines. The PNVG consists only of links marked by thick lines [see Fig. 1(b)].

A formal description of the PNVG mapping algorithm is as follows:

(1) To build the NVG acc. to [21] using standard NVG criterion for mapping

$$\left\{(i,j) \in NVG, x(t_k) < x(t_i) + (x(t_j) - x(t_i)) \times \frac{t_k - t_i}{t_j - t_i},\ i < k < j\right\}, \tag{1}$$

where i and j are numbers of two arbitrary time events $t_i < t_j$ and t_k is any event between them $t_i < t_k < t_j$.

(2) To set for every link of NVG the direction and the weight (the angle of view).

All the NVG links are attributed to the natural temporal direction, i.e., the link (i,j), $i < j$ is considered to be directed from i to j. The weight is the angle on the time series plot between downward direction and direction of the line going from $x(t_i)$ to $x(t_j)$ [see Fig. 1(a)]

$$\alpha_{ij} = \text{arctg}\frac{x(t_j) - x(t_i)}{t_j - t_i}, \quad i < j. \tag{2a}$$

(3) To select links from the above created directed and weighted graph according to the rule that uses introduced arbitrary parameter—the angle of view α, $0 \leqslant \alpha \leqslant \pi$:

$$\{(i,j) \in \text{PNVG}(\alpha), \quad \alpha_{ij} < \alpha\}. \tag{2b}$$

One can find from rules 1–3 that the PNVG(α) is a directed acyclic graph, the PNVG(α) can be either a connected or disconnected graph.

In the present work PNVG(α) is constructed for three artificial and three experimental time series. Artificial time series have the following distributions of intervals: the uniform random distribution (3a), the Poisson distribution (3b), and the Weierstrass distribution (3c) having a fractal dimension D. Let $\{r_i,\ i = 1,\ldots,N+1\}$ be a random variable uniformly distributed on the interval $[0,1]$:

$$d_i = r_i, \quad t_1 = 0, \quad t_i = t_{i-1} + d_{i-1}, \quad x(t_i) = d_i, \tag{3a}$$

$$d_i = -1/\lambda \ln(r_i), \quad t_1 = 0, \quad t_i = t_{i-1} + d_{i-1}, \quad x(t_i) = d_i \tag{3b}$$

$$d_i = \sqrt{2}\sigma \frac{\sqrt{1 - b^{2D-4}}}{\sqrt{1 - b^{(2D-4)(M+1)}}} \times \sum_{m=0}^{M} \{b^{(D-2)m} \sin[2\pi(sb^m i + r)]\}$$

$$t_1 = 0, \quad t_i = t_{i-1} + |d_i|, \quad x(t_i) = d_i. \tag{3c}$$

The following parameter values are chosen: for the Poisson distribution (3b) $\lambda = 1$, for the Weierstrass distribution (3c) $D = 1.3$, $\sigma = 3.3$, $b = 2.5$, $s = 0.005$, $M = 10$, the modulus in (3c) was used because the Weiesrstrass distribution is alternating.

II. THE RELATIVE NUMBER OF CLUSTERS AS THE ORDER PARAMETER

All possible properties of NVG can be calculated also for PNVG [38]. For example, the average node degree, the clustering coefficient, etc. Such PNVG parameters become dependent on the angle of view, however, there are properties unique to the PNVG.

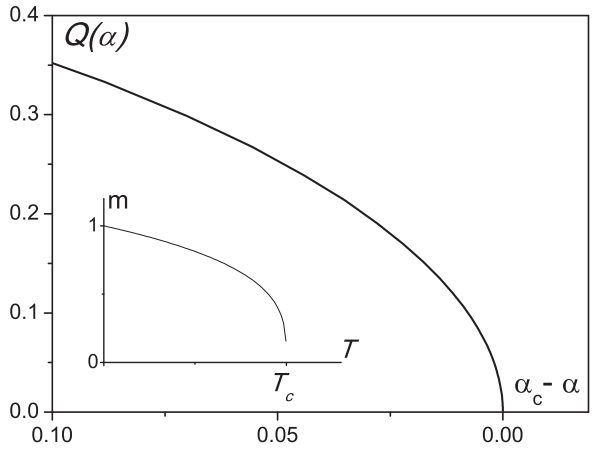

FIG. 2. The relative number of clusters $Q(\alpha)$ for uniformly distributed time series (3a). In the inset the order parameter $m(T)$ of the second-order phase transition as a function of temperature T, T_c is the critical temperature.

The relative number of clusters $Q(\alpha)$ is the number of clusters in PNVG (α) divided by the total number of nodes N in the graph. The cluster is a set of interconnected nodes of the graph, a single node is also considered as a cluster.

The relative number of clusters in the PNVG(α) also depends on α but this property does not exist for the NVG because the NVG always consists of one and only one cluster.

The PNVG (α) with a small, looking downward angle of view (see Fig. 1) consists of N single node clusters, therefore $Q(\alpha < \pi/4) = 1$. Beginning from $\alpha = \pi/4$ the PNVG algorithm generates links, new multinode clusters are emerging, and the relative number of clusters $Q(\alpha)$ gradually decreases. Finally, at the zenith angle of view $\alpha = \pi$ all the clusters merge into one and $Q(\alpha = \pi) = 1/N$, in other words, for large N one always get $Q(\alpha = \pi) \approx 0$. The numerical simulations show that the relative number of clusters tends to zero $Q(\alpha \to \pi/2) \to 0$ already at $\alpha \to \pi/2$.

Figure 2 shows $Q(\alpha)$ for time series with the uniform distribution (3a) and in the inset a schematic behavior of the spontaneous magnetization of a ferromagnet as a function of temperature is presented. At a certain temperature T_c (the Curie temperature) the specific magnetization $m(T)$ becomes zero [39] and the ferromagnet becomes the paramagnet. Such a transition is called a second-order phase transition. The temperature T_c at which this transition occurs is called the critical temperature (the critical point) and the $m(T)$ is called the order parameter.

Figure 2 reveals that at a certain critical angle of view $\alpha_c = \pi/2$, the PNVG (α_c) has almost all the nodes interconnected and it consists of several clusters, hence $Q(\alpha \geqslant \alpha_c) \approx 0$ for large N.

The order parameter has a power-law behavior (4) near the critical point when the size of the investigated system is greater than the correlation length. The corresponding so-called critical exponent or critical index β is the main parameter of the second-order phase transition:

$$m(T) \sim (-t)^{\beta}, \quad t = (T - T_c)/T_c, \tag{4}$$

where $t = (T - T_c)/T_c$ is the proximity to the critical point of phase transition.

Similar behavior is demonstrated by many other systems like antiferromagnets, ferroelectrics (where the order parameter is the spontaneous electric polarization), the transition of liquid helium in the superfluid state, etc.

According to Landau's mean field theory [39], the value of the index is $\beta = 1/2$. In this theory the fluctuations of the order parameter are ignored. Ginzburg and Levanyuk [39] introduced the criterion of applicability of Landau's theory. In some systems, the criterion is met, for example, for the superconducting transition and, accordingly, $\beta = 1/2$. In the cases when the criterion is not met, the theory of phase transitions becomes more complicated and critical exponents cannot be found exactly. In this case the critical index value of the order parameter is approximately $\beta \approx 0.3$.

The proximity to the critical angle of view α_c will be denoted further by $\tau = (\alpha - \alpha_c)/\alpha_c$. The $Q(\tau)$ was calculated numerically for artificial time series (3a)–(3c) having $N = 10^5$ intervals. Figure 3(a) shows the results obtained by averaging ten different generated time series of each type (3a)–(3c). The error of each data point presented in Fig. 3(a) is less than 3%. Critical indices and their errors are listed in Table I.

Figure 3(b) presents $Q(\tau)$ for the experimental time series. The time series of RR intervals of healthy human cardiac rhythm were taken from [40]. Plotted data were obtained by averaging 25 RR series (nsr01–nsr25 acc. to [40]), the length of

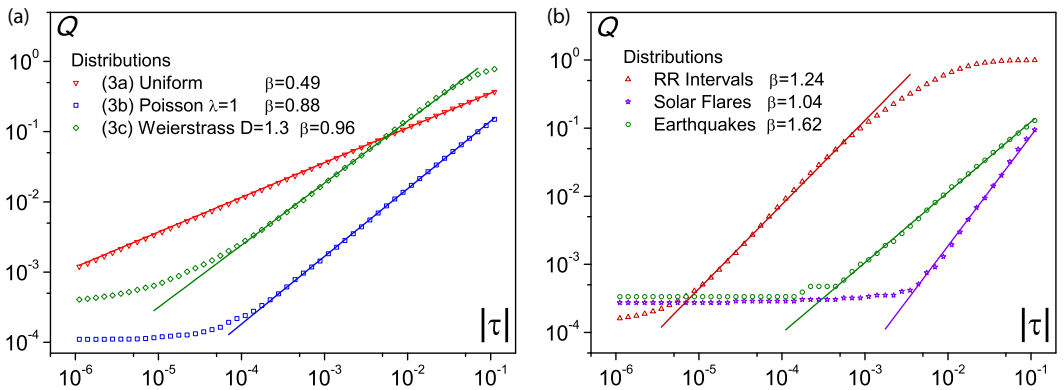

FIG. 3. The relative number of clusters Q upon the proximity to the critical angle $\tau = (\alpha - \alpha_c)/\alpha_c$ in a log-log scale. (a) Artificial time series (3a)–(3c). (b) Experimental time series: RR intervals of healthy human cardiac rhythm, solar flares, and seismic activity.

TABLE I. Critical exponents, calculated.

Distribution	Critical exponent		
	β	ϑ	$\nu = \beta/\vartheta$
Uniform distribution (3a)	0.49 ± 0.02	0.88 ± 0.04	0.56 ± 0.04
Poisson distribution (3b)	0.88 ± 0.03	0.87 ± 0.05	1.01 ± 0.06
Weierstrass distribution (3c)	0.96 ± 0.09	0.92 ± 0.08	1.04 ± 0.13
RR intervals of healthy human cardiac rhythm [49]	1.24 ± 0.08	0.83 ± 0.08	1.49 ± 0.17

RR-intervals time series varied in the range $6-11 \times 10^5$. Time series of the solar flares beginnings was observed in 2002–2012 by the HESSI project [41], more than 6×10^4 flares. Also the time series of the earthquakes with a magnitude higher than 3.5 on the Richter scale occurring in 1960–2010 was based on [42], the length of series is more than 2×10^4 events.

For all the above time series the $Q(\tau)$ demonstrates the power-law behavior and allows us to obtain the critical exponent

$$Q(\tau) \sim (-\tau)^{\beta}, \quad \tau = (\alpha - \alpha_c)/\alpha_c, \quad \alpha < \alpha_c. \tag{5}$$

The critical exponents β (5) were calculated on the base of data presented in Fig. 3. The lowest calculated value of the critical index $\beta = 0.49 \pm 0.02$ has artificial time series with the uniform distribution (3a), the value coincides with β of Landau's mean field theory [39]. Critical indices of all other distributions both artificial (3b) and (3c) and experimental were higher (see Table I).

It can be shown that $\beta = 1/2$ for the time series generated by the uniform random distribution (3a). To justify it, we assume that the clusters in the PNVG(α), having a certain average size, are formed with equal probability irrespective of $\tilde{\alpha}$, the deviation from the critical angle of view $\alpha_c, \tilde{\alpha} = \alpha_c - \alpha$, $\tilde{\alpha} \ll 1$. To simplify the calculations, we assume also that the distance between nodes (see Fig. 1 and the description of the PNVG algorithm) is the constant equal to 1.

This allows us to find the probability of emerging of the cluster with the average size L at the angle $\tilde{\alpha}$ as the product of probabilities that each next node has to be shorter for not less than the $tg\,\tilde{\alpha}$ value (see Fig. 1), i.e.,

$$P(\tilde{\alpha}, L) = \frac{1}{2^L} \prod_{n=1}^{L} (1 - ntg\tilde{\alpha}). \tag{6}$$

According to the first assumption $P(\tilde{\alpha}, L) = P(k\tilde{\alpha}, L_k)$, where $k > 1$ and L_k is the average length of a cluster at the angle $k\tilde{\alpha}$. In this way we get

$$\frac{1}{2^L} \prod_{n=1}^{L} (1 - ntg\,\tilde{\alpha}) = \frac{1}{2^{L_k}} \prod_{n=1}^{L_k} (1 - ntg\,k\tilde{\alpha}). \tag{7}$$

Furthermore, by performing logarithm (7) and taking into account that $tg\,\tilde{\alpha}$ at small angles $\tilde{\alpha} < k\tilde{\alpha} \ll 1$ has the value of $tg\,\tilde{\alpha} \approx \tilde{\alpha}$ and considering terms with the highest power of $\tilde{\alpha}$ in obtained relations we get $\tilde{\alpha} L^2 = k\tilde{\alpha} L_k^2$ and correspondingly

$$\frac{L}{L_k} = \sqrt{k}. \tag{8}$$

Thus, the ratio of the average cluster sizes in the PNVG does not depend on the angle of view. The number of clusters is inversely proportional to their size, respectively, $\beta = 1/2$ which corresponds to the above presented numerical simulation results.

III. PHASE TRANSITION NEAR CRITICAL POINT

Another feature of the $Q(\tau)$ behavior at $|\tau| \ll 1$ can be seen from Fig. 3—$Q(\tau)$ is independent on τ at $|\tau| \to 0$ in the Δ area near the critical point when α approaches α_c. The theory of the second-order phase transitions [39] predicts such behavior of the order parameter in the proximity to the critical point. The presence of so-called external field h causes such an effect. The order parameter in the above case depends only on h,

$$m(t) \sim h^{1/\delta}. \tag{9}$$

Note that at the external field $h > 0$ the order parameter $m(t)$ above the critical point $t > 0$ ($T > T_c$) is not zero and depends on t,

$$m(t) \sim h t^{-\gamma}. \tag{10}$$

There is the relation between critical exponents above β, below γ critical point and δ is the exponent on the critical point [39,43,44], i.e., Widom relation [45]

$$\beta\delta = \beta + \gamma. \tag{11}$$

The size of the area near the critical point Δ can be found from the condition that the values of the order parameter $m(t)$ above and below the phase transition point are equal:

$$\Delta^{\beta} = h\Delta^{-\gamma}, \quad \Delta = h^{\frac{1}{\beta+\gamma}}. \tag{12}$$

Different experimental time series [Fig. 3(b)] have different Δ sizes, which are determined by the time series nature and the measurement accuracy of studied time series.

Consider the effect of measurement accuracy on $Q(\alpha)$ using the time series with the uniform distribution (3a). Let us convert initial (3a) time series $x(t_i)$ to the series with only M different values or levels by a simple transformation $\tilde{x}(t_i, M) = ceil(x(t_i)M)/M$, where M is the number of sampling levels, $ceil(a)$ rounds a upward. Smaller M means that $\tilde{x}(t_i, M)$ is a rougher approximation of $x(t_i)$ time series. For example, if $M = 2$ then the time series $\tilde{x}(t_i, M)$ contains only two values $1/2$ and 1.

Figure 4 shows the shapes of $Q(\tau)$ for uniformly distributed (3a) time series for different sampling levels M. The manner of how the $\Delta(M)$ values are found is schematically plotted in Fig. 4(a) and calculated data are presented in Fig 4(b). The $\Delta(M)$ has power-law behavior with critical

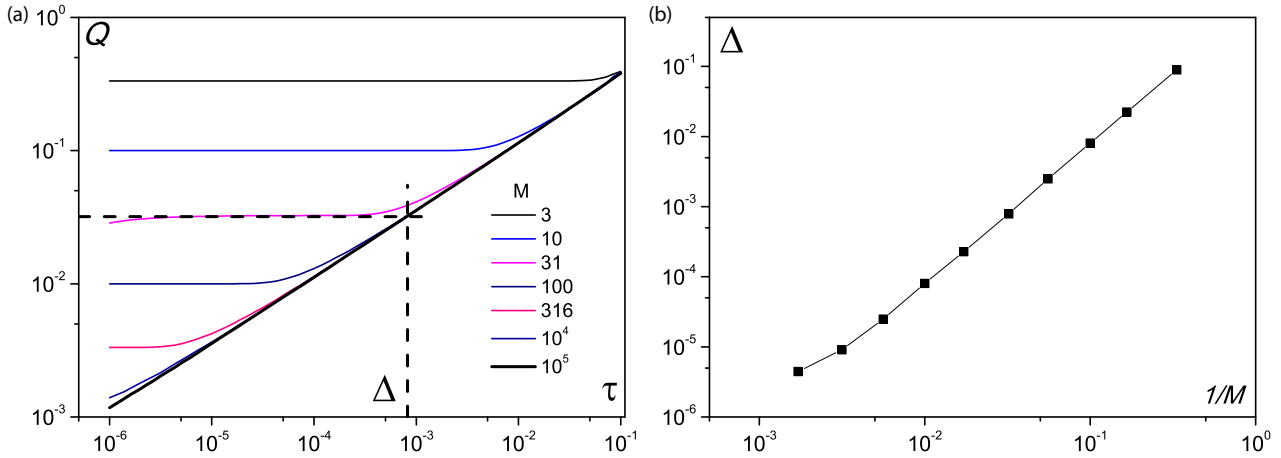

FIG. 4. The influence of sampling levels number M on (a) the relative number of clusters $Q(\tau)$ for the uniform distribution (3a) time series and (b) the size of the area near the critical point Δ upon the inverse of sampling levels $1/M$.

exponent Ω,

$$\Delta = (1/M)^{\Omega}, \quad \Omega = 1.98 \pm 0.04, \tag{13}$$

where, of course, the Ω is given for the uniformly distributed (3a) time series.

Also as it follows from Fig. 4(a), the value $Q(\tau, 1/M)$ at $|\tau| \leqslant \Delta$ relates to $1/M$ in a simple way:

$$Q(|\tau|, 1/M) = 1/M. \tag{14}$$

Thus, on the one hand, from (14) and (13) we get

$$Q(|\tau| \leqslant \Delta) = \Delta^{1/\Omega}, \tag{15}$$

and, on the other hand, according to (5),

$$Q(|\tau| = \Delta) = \Delta^{\beta}, \tag{16}$$

which implies that the critical exponents Ω and β relates as follows:

$$\Omega = 1/\beta. \tag{17}$$

Equation (17) is in conformity with the numerical experiments which gives $\Omega = 1.98 \pm 0.04$ (13) and $\beta = 0.49 \pm 0.02$ for time series with random uniform distribution (3a).

The relationship between $1/M$ and external field h can be found also. According to (12) and (13) we obtain

$$(1/M)^{\Omega} = h^{\frac{1}{\beta+\gamma}}, \tag{18}$$

where, in view of (17)

$$h = (1/M)^{\Omega(\beta+\gamma)} = (1/M)^{\frac{\beta+\gamma}{\beta}}. \tag{19}$$

When $h \neq 0$ the order parameter above the critical point is not equal to zero and it has to demonstrate a power-law behavior (10) upon the proximity to the critical point. The critical index γ, which describes the behavior of Q above α_c:

$$Q(\tau > 0, h \neq 0) \sim \tau^{-\gamma}. \tag{20}$$

The numerical simulation for the random uniform distribution time series (3a) gives

$$\gamma = 0.097 \pm 0.008. \tag{21}$$

IV. FINITE SIZE SCALING: $L \leqslant \xi$

The case when the size of the system L is less or of the same order as the correlation length ξ changes the behavior of the order parameter, for example, $m(T)$ at $T = T_c$ (more correctly, inside the Δ area near the critical point [39]). The relationship (4) has to be replaced with the relation [46]

$$m(L) \sim L^{-\vartheta}, \quad \vartheta = \beta/\nu, \tag{22}$$

where ϑ is the critical exponent of the finite size scaling and ν is that of the correlation length

$$\xi \sim |T_c - T|^{-\nu}. \tag{23}$$

Such behavior of the order parameter $m(T)$ is called a finite size scaling. In the case when the size of the system $L \gg \xi$, any measured system property does not depend on the system samples, i.e., the properties of the system are self-averaged. In the opposite case, when $L \leqslant \xi$, the order parameter $m(T)$ has to be found as a time or sample averaged value. For the PNVG this means that for $L \leqslant \xi$ the relative number of clusters Q has to be calculated as the average value over the system samples.

Having known the critical exponent β (6) and the critical exponent of the finite size scaling ϑ (22) one can find the critical exponent of the correlation length [39]

$$\nu = \beta/\vartheta. \tag{24}$$

Another verification of the fact that Q is the order parameter analog, is the fact that for the short $N < \xi$ time series Q behaves as

$$Q(\tau = 0, N) \sim N^{-\vartheta}, \tag{25}$$

where N is the length of the time series and ϑ is the critical index of finite size scaling of Q.

Values of $Q(\tau = 0, N)$ are calculated numerically for the artificial time series (3a)–(3c) and for the time series of RR intervals of healthy human cardiac rhythm Fig. 5.

The time series of RR intervals of healthy human cardiac rhythm were obtained from the 24 time series of RR intervals (nsr26–nsr50 acc. to [40]) by sequentially slicing them into

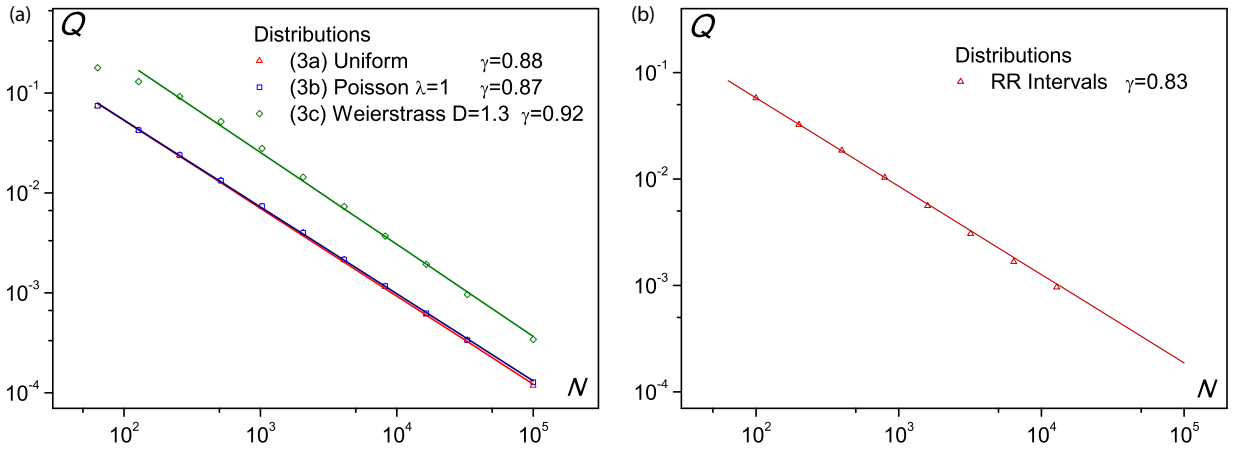

FIG. 5. The plot of $Q(\tau = 0, N)$ upon the length of the time series N. (a) Artificial time series (3a)–(3c). (b) RR intervals of healthy human cardiac rhythm.

pieces of certain length without overlays. The results of calculations of the critical exponents are presented in Table I.

Calculated critical exponents ϑ of $Q(\tau \leqslant \Delta, N)$ depend upon the nature of the time series weakly, while the exponents β strongly depend on the time series (see Table I). Thus, the appropriate critical exponents of the correlation length ν (7) depend strongly on the original time series nature [38].

V. DISCUSSION

In this study we found that the behavior of the relative number of clusters $Q(\tau)$ in the graphs produced by the PNVG algorithm has the same behavior as the order parameter in the theory of the second-order phase transitions. It is argued by the following important facts.

First, there exists the critical point at the angle of view $\alpha_c = \pi/2$. Near the critical point the relative number of clusters $Q(\tau)$ demonstrates the power-law dependence upon the proximity to the critical point $\tau = (\alpha - \alpha_c)/\alpha_c$. Critical exponents of $Q(\tau)$ above β and below γ the critical point $\alpha_c = \pi/2$ are calculated.

Second, the $Q(\tau)$ value depends on the length of the time series to a power law when the length of the time series is less than the correlation length of the PNVG, as it should be in the theory of the second-order phase transitions.

Third, inside the area near the critical point, the presence of the external field analog h originates the $Q(\tau)$ to be independent on τ but the power law dependent on h.

Fourth, the numerical values of the critical exponents satisfy the basic Widom [45] relation.

All of these patterns can be concisely formulated as the scaling hypothesis (relation).The relative number of clusters $Q(\tau, h)$ depends on two variables: τ the proximity to the critical point, and h the external field

$$Q(\tau, h) = h^{1/\delta} f(\tau/h^{1/\beta\delta}) \tag{26}$$

and can be expressed also in the form of the scaling function $f(z)$ of the single variable which has following forms of asymptotic behavior:

$$f(z \to -\infty) \sim (-z)^{\beta}, \quad f(z \to 0) = \text{const}, \quad f(z \to +\infty) \sim z^{-\gamma}, \tag{27}$$

where

$$\beta\delta = \beta + \gamma. \tag{28}$$

Up to notation the relations (26)–(28) match those in the theory of the second-order phase transitions.

Note that the (26)–(28) take place in the percolation theory [47,48] also, where the role of the order parameter is played by the density of the infinite cluster $P(\tau, h)$, where $\tau = (p - p_c)/p_c$, p is the concentration of connected links (nodes) and the external field h is associated with the Kasteleyn-Fortuin demon [49].

The conductivity of a randomly inhomogeneous medium near the percolation threshold with different phase

TABLE II. Critical exponents.

Systems with the second-order phase transition		Critical exponent			
		β	γ	δ	ν
PNVG (current study)		0.49	0.10	1.18	0.56
The Landau's mean field theory		1/2	1	3	1/2
Fluctuation theory of the second-order phase transition	3D	1/3	4/3	5	2/3
Percolation theory	2D	5/36	43/18	18.14	1/33
	3D	0.41	1.80	4.78	0.88
Effective conductivity in percolation structure[a]	2D	1.3	1.3	2	1.33
	3D	2	0.72	1.36	0.88

[a]In the effective conductivity theory exponents β and γ are denoted as t and q, respectively.

conductances $\sigma_1 \gg \sigma_2$ behaves in the same way as (26)–(28). The role of the order parameter plays the normalized effective conductivity $\sigma_{\text{eff}}(\tau,h)/\sigma_1$ and the external field is the ratio of phase conductivities $h = \sigma_2/\sigma_1$. Critical exponents of systems with the second-order phase transition that are mentioned above are listed in Table II.

VI. CONCLUSIONS

The use of the algorithm of mapping time series to the complex networks (graphs) particularly to the parametric natural visibility graphs allows us to discover and explore properties of time series including those originated by the parametric graphs features. The property investigated in this study—the relative number of clusters in such a graph demonstrates the scaling behavior and characterized by a set of critical exponents satisfying the Widom relation.

Critical exponents above and below the critical point for the relative number of clusters in the parametric visibility graphs were calculated as well as the exponents in the finite size scaling regime. Altogether, this allowed us to find the critical exponents of the correlation length for generated graphs.

As a result, the similarity is found between the behavior of the relative number of clusters in the parametric visibility graphs and the order parameter in the second-order phase transitions theory.

Thus, we added to the list of systems with observed second order phase transition—magnetic systems, binary mixtures, alloys, superfluidity and superconductivity, percolation (geometrical and "physical") a new system—the parametric natural visibility graphs.

[1] C. Liu, W.-X. Zhou, and W.-K. Yaun, Physica A **389**, 2675 (2010).
[2] M.-C. Qian, Z.-Q. Jiang, and W.-X. Zhou, J. Phys. A **43**, 335002 (2010).
[3] Z.-G. Shao, Appl. Phys. Lett. **96**, 073703 (2010).
[4] X. Li and Z. Dong, Phys. Rev. E **84**, 062901 (2011).
[5] L. Lacasa, B. Luque, J. Luque, and J. C. Nuño, Europhys. Lett. **86**, 30001 (2009).
[6] L. Lacasa and R. Toral, Phys. Rev. E **82**, 036120 (2010).
[7] B. Luque, L. Lacasa, F. J. Ballesteros, and A. Robledo, PLoS ONE **6**, e22411 (2011).
[8] B. Luque, L. Lacasa, F. J. Ballesteros, and A. Robledo, Chaos **22**, 013109 (2012).
[9] G. Gutin, T. Mansour, and S. Severini, Physica A **390**, 2421 (2011).
[10] J.-F. Zhang and Z.-G. Shao, Indian J. Phys. **85**, 1425 (2011).
[11] A. Nuñez, L. Lacasa, E. Valero, J. Patricio, and B. Luque, arXiv:1108.1693.
[12] A. M. Nuñez, L. Lacasa, J. P. Gomez, and B. Luque, in *New Frontiers in Graph Theory*, edited by Y. Zhang (InTech, Shanghai, 2012), p. 119.
[13] L. Lacasa, A. Nuñez, E. Roldan, M. R. Parrondo, and B. Luque, Eur. Phys. J. B **85**, 217 (2012).
[14] L. Telesca, M. Lovallo, and J. O. Pierini, Chaos Solitons Fractals **45**, 1086 (2012).
[15] J. B. Elsner, T. H. Jagger, and E. A. Fogarty, Geophys. Res. Lett. **36**, L16702 (2009).
[16] J. Tang, F. Liu, W. Zhang, S. Zhang, and Y. Wang, Physica A **450**, 635 (2016).
[17] A. K. Charakopoulos, T. E. Karakasidis, P. N. Papanicolaou, and A. Liakopoulos, Phys. Rev. E **89**, 032913 (2014)
[18] A. K. Charakopoulos, T. E. Karakasidis, P. N. Papanicolaou, and A. Liakopoulos, Chaos **24**, 024408 (2014)
[19] I. A. Fuwape, S. T. Ogunjo, S. S. Oluyamo, and A. B. Rabiu, Theor. Appl. Climatol, 1 (2016).
[20] J. Zhang and M. Small, Phys. Rev. Lett. **96**, 238701 (2006).
[21] L. Lacasa, B. Luque, F. Ballesteros, J. Luque, and J. C. Nuño, Proc. Natl. Acad. Sci. U.S.A. **105**, 4972 (2008).
[22] B. Luque, L. Lacasa, F. Ballesteros, and J. Luque, Phys. Rev. E **80**, 046103 (2009).
[23] C.-K. Peng, S. V. Buldyrev, S. Havlin, M. Simons, H. E. Stanley, and A. L. Goldberger, Phys. Rev. E **49**, 1685 (1994).
[24] C.-K. Peng, S. Havlin, H. E. Stanley, and A. L. Goldberger, Chaos **5**, 82 (1995).
[25] A. L. Goldberger, L. A. N. Amaral, J. M. Hausdorff, P. C. Ivanov, and C.-K. Peng, Proc. Natl. Acad. Sci. U.S.A. **99**, 2466 (2002).
[26] M. Costa, A. L. Goldberger, and C.-K. Peng, Phys. Rev. Lett. **89**, 068102 (2002).
[27] H. Kantz and T. Schreiber, *Nonlinear Time Series Analysis* (Cambridge University Press, Cambridge, 2003).
[28] A. C.-C. Yang, S.-S. Hseu, H.-W. Yien, A. L. Goldberger, and C.-K. Peng, Phys. Rev. Lett. **90**, 108103 (2003).
[29] M. Costa, A. L. Goldberger, and C.-K. Peng, Phys. Rev. Lett. **95**, 198102 (2005).
[30] M. Small, *Applied Nonlinear Time Series Analysis* (World Scientific, London, 2005).
[31] R. Albert and A.-L. Barabási, Rev. Mod. Phys. **74**, 47 (2002).
[32] S. N. Dorogovtsev and J. F. F. Mendes, *Evolution of Networks. From Biological Nets to the Internet and WWW* (Oxford University Press, Oxford, 2003).
[33] M. E. J. Newman, SIAM Rev. **45**, 167 (2003).
[34] S. Bocaletti, V. Latora, Y. Moreno, M. Chavez, and D.-U. Hvang, Phys. Rep. **424**, 175 (2006).
[35] A. Barrat, M. Barthelemy, and A. Vespignani, *Dynamics Processes on Complex Networks* (Cambridge University Press, Cambridge, 2008).
[36] S. N. Dorogovtsev, A. V. Goltsev, and J. F. F. Mendes, Rev. Mod. Phys. **80**, 1275 (2008).
[37] M. E. J. Newman, *Networks: An Introduction* (Oxford University Press, Oxford, 2010).
[38] A. Snarskii and I. Bezsudnov, Physica A **414**, 53 (2014).
[39] L. D. Landau and E. M. Lifshitz, *Statistical Physics, Third Edition, Part 1: Volume 5* (Elsevier, New York, 2013).
[40] A. L. Goldberger, L. A. N. Amaral, L. Glass, J. M. Hausdorff, P. Ch. Ivanov, R. G. Mark, J. E. Mietus, G. B. Moody, C.-K. Peng, and H. E. Stanley, Circulation **101**, e215 (2000).

[41] http://hessi.ssl.berkeley.edu/data.
[42] *Annual Earthquakes in the USSR (ESSN)* (Nauka, Moscow, 1962–1994).
[43] S.-K. Ma, *Modern Theory of Critical Phenomena* (Perseus, Cambridge, MA, 2000).
[44] A. Z. Patashinskii and V. L. Pokrovskii, *Fluctuation Theory of Phase Transitions* (Pergamon, New York, 1979).
[45] B. Widom, J. Chem. Phys. **43**, 3898 (1965).
[46] K Christensen and N. R. Moloney, *Complexity and Criticality* (Imperial College Press, London, 2005).
[47] D. Stauffer and A. Aharony, *Introduction to Percolation Theory* (Taylor and Francis, London, 1992).
[48] B. I. Shklovskii and A. L. Efros, *Electronic Properties of Doped Semiconductors* (Springer, Berlin, 1984).
[49] P. W. Kasteleyn and C. M. Fortuin, J. Phys. Soc. Jpn. Suppl. **26**, 11 (1969).